Masters Theses   Graduate School

8-2021

Development of A Point-of-Use Testing Platform for Detecting Bacteria Infection in Raw Milk

Xin Xia
University of Tennessee, Knoxville, xxia6@vols.utk.edu

Recommended Citation

To the Graduate Council:

I am submitting herewith a thesis written by Xin Xia entitled "Development of A Point-of-Use Testing Platform for Detecting Bacteria Infection in Raw Milk." I have examined the final electronic copy of this thesis for form and content and recommend that it be accepted in partial fulfillment of the requirements for the degree of Master of Science, with a major in Electrical Engineering.

Jie Wu, Major Professor

We have read this thesis and recommend its acceptance:

Gu Gong, Qing Cao

Accepted for the Council:
Dixie L. Thompson

Vice Provost and Dean of the Graduate School

(Original signatures are on file with official student records.)

Development of A Point-of-Use Testing Platform for Detecting Bacteria Infection in Raw Milk

A Thesis Presented for the

Master of Science

Degree

The University of Tennessee, Knoxville

Xin Xia

August 2021

To my fortitudinous parents who support me all the way along, my gracious sister, and my trusty seniors and friends.

Acknowledgments

I would like to thank my advisor Dr. Jie "Jayne" Wu who has guided me patiently through these two years. During the pandemic, she has given me much reassurance and support. She accepted my flaw and help me overcome difficulties in research. This work could not be done without any of her efforts.

I would also like to thank Dr. Gong Gu, Dr. Qing "Charles" Cao, who have delivered the best lectures. They willingly serve as my thesis and defense committee members They always respond to my questions immediately. Their challenging questions and thoughtful explanations are what stimulate my further explorations. Their magnanimity is what I do not deserve.

I would like to take a bow figuratively and thank Dr. Shigetoshi Eda, and his research assistants in Department of Forestry, Wildlife and Fisheries. Their support helps me through many unfamiliar subjects. Their perseverance tells me the importance of good practices and patience.

Yu and Jiamei took me in as a workmate and as a beloved young brother. I would like to thank them for their love and care. Most importantly, I would like to thank my parents and sister, Fei. They have been always encouraging me through their caring and soothing voices. Let alone their tremendous financial sacrifices.

Abstract

The detection and quantification of bacteria are essential to environment and food quality monitoring. Escherichia coli (E. coli) is a common pathogen, also a causative agent of mastitis. Traditional methods usually require samples to be tested in a laboratory. However, sending samples to remote lab increases the cost of time and money spent on delivery. Sometimes, samples can degrade during this long progress and cause inaccuracy. A low cost and reusable sensor is designed to perform on-site quantification. The sensor composed of two layers of asymmetrical mesh electrodes, which is used in coordination magnetic microparticles functionalized with bacterium-specific antibody. Immunological binding between the bacteria and its antibody is utilized to identify the target. The sensor can selectively detect coagulated clusters of bacteria and magnetic microparticles, which is based on negative dielectrophoresis and alternating current electrothermal microflows. A hypothesis is proposed and experimentally validated to explain the sensing mechanism, which is used to improve the detection sensitivity. Further, a compact and embedded testing kit (aceTeK) is developed to help perform point-of-use testing and diagnosis. Data is acquired, processed, and analyzed to yield a conclusion about the existence of any bacteria infection in the milk.

Table of Contents

List of Tables

List of Figures

Chapter 1

Introduction

This work investigates on-site bacteria detection during milk production. Fast and online detection helps monitor the quality of the product and discover possible bovine mastitis as well. To resolve the challenges in the traditional methods, a mesh sensing device is introduced with explanation of its mechanism. The other key part of this system is the embedded testing system. Its performance is further demonstrated later in the following sections.

1.1   Research Background

Bovine mastitis has caused a loss of profit in milk industry. It brings down the total product milk yield. When mastitis happens to cows, the inflammatory symptom causes the quality of milk severely damaged, for example, the color can change, as shown in Fig. 1.1, and clots may form.

Early detection and discovery help save cows from health problem, so that more nutrition can be converted into milk while less money needs to be spent on medicine. There are reports of finding bacteria in the milk from infected cows[1]. Hence, one of the most direct method to find the sign of mastitis is to detect the bacteria infection in the milk samples. Since the cause of mastitis is leukocyte-related immune dysfunction, the detection of disease can also be achieved through checking the level of white blood cells[9]. In-lab E. coli detection has been developed with very low LOD for a long time, but few of them can really work on site

and perform diagnosis of the disease. Portable on-site detection devices can help diagnose and even prevent bovine mastitis.

1.2 Sensing Devices

1.2.1 Sensor Review

To better understand the current development of bacteria detection, recent sensors are discussed in this sub-section. These sensors utilize electrical signals and could potentially be put into a small detection device.

Affinity sensors are popular in bacteria and chemical sensing for their versatility of different surface chemical structures. They often have certain kind of probes immobilized on the surface of gold electrode[13, 14]. The detection time typically varies from 1 to 2 hours. They have low LODs around 10^2 CFU/mL, which is around 10^3 cells/mL because not all cells can grow into colonies while sometimes multiple cells can grow into one big colony. The electrical signals used for detection includes the change rate of capacitance and impedance. Electrodes modified with biochemical probes sometimes need to be kept in low temperature before use[13]. This could lead to difficulty of transportation all along in cold chain. The other problem is that when using electrochemical sensing, there are always reference electrode and working electrode involved with a potentiostat[13, 6]. This is good for accuracy, but not suitable for portable testing platform.

There must be a process of binding or conjugating when the specificity is the feature of the sensor. Apart from affinity sensors, this process can also happen before the sensing step. Some impedance or capacitance sensors can distinguish conjugated and non-conjugated samples[12]. These sensors tend to become intricate in its structure, since they need to generate certain kind of force field. Some use elaborated microfluidics and channels to separate the target particles from the background[4]. It requires a syringe pump system with speed control other than the electrical detection platform to move the particles. But one obvious advantage of these sensors is that the binding process only exist for the target

2

samples, not for any electrode surface. There is no need to design specific chemical structure for binding with or linking to the surface.

1.2.2 Overview of Mesh Device

The sensor used in this work is asymmetrical mesh device, asymmetrical being mainly the opening percentage of the top mesh layer is a lot bigger than what it is in the one under, separated by spacers. Target particles will be let in from the top and trapped in between, inducing changes in capacitance. Since the device is made out of tapes and stainless mesh strips, low cost of raw materials and process technology can be expected.

1.3 Testing Platform Design Goals

The aceTeK testing platform is based on an ARM SoC hardware running an IoT system developed also by ARM. Its easy programming style and abundant developing resources helps reduce the time of programming and debugging. The hardware board has provided all that is needed in a sensing circuit.

In PCB electrode, a signal small as 5 mVrms is enough to attract big targets like bacteria to the surface, then binding with the deposited antibody or single strained DNA aptamer. Since it is using positive DEP force, the frequency is supposed to be as high as 100 kHz.

On the other side, a mesh device only requires a working frequency at 1 kHz according to optimization experiments in the later section. But meanwhile, revealed in the same set of experiments, the amplitude must be as high as 1 Vrms.

These two kinds of devices are like two extremes, deciding the design goals of this testing platform. Along with other requirement, a more detailed form is listed below.

1.4 Contribution

There are two main aspects discussed in this thesis. One is the mesh device. The other is the compact testing platform.

3

This work proposed a mesh device with structure reinforcement. It can be used for multiple times. With external fluid system, it can be easily clean and reset[15]. The cost is super low since the main materials are stainless steel meshes and common scotch tapes. To reach the goal of detection with specificity, magnetic beads are introduced to bind with specific targets. This method is versatile for all kind of particles, as long as there is an efficient corresponding antibody.

To comply with the requirement of on-site sensing, a small low-powered mobile testing platform is developed. The footage can be as small as several coins of a quarter. The platform can reach a very small voltage down to 5 mVrms, which can be used in nano-molecule detection[8], as well as a high voltage of 1 Vrms for mesh sensors.

The test result can prove the ability to detect bacteria, even in complicated solution backgrounds. This enhances the possibility for uses in different complex fields.

4
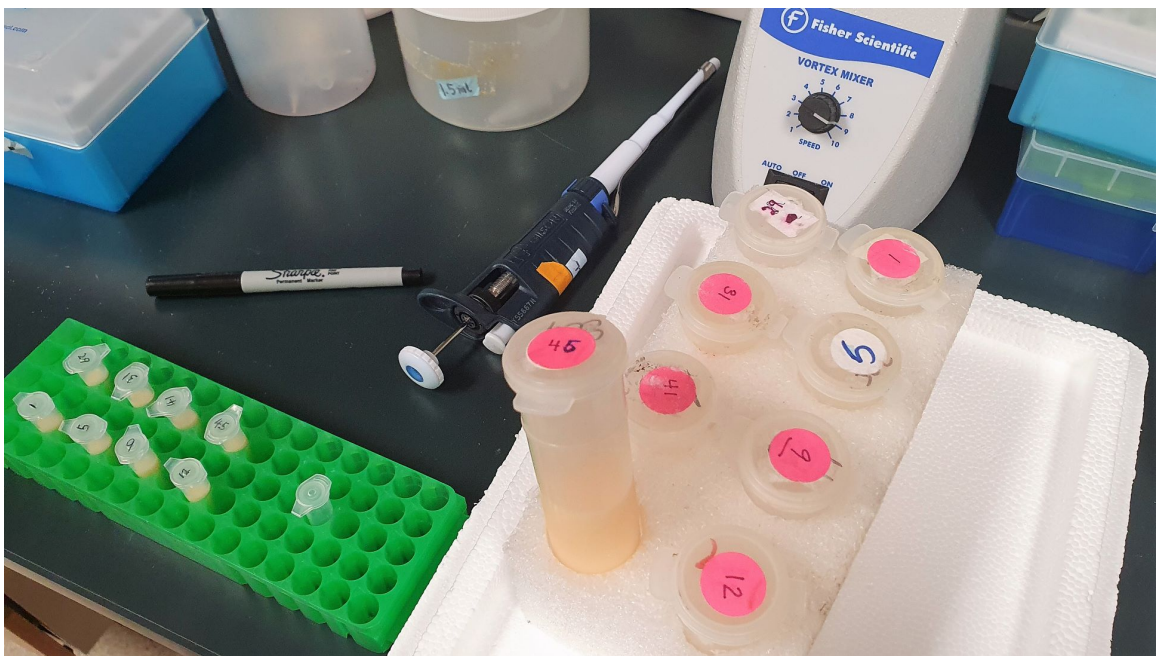
Figure 1.1: Samples of milk affected by mastitis, obtained from DHIA through Animal Science, UTIA.

Chapter 2

ACEK Sensing Theory

2.1 Basic AC Electrokinetics (ACEK) Theory

ACEK uses alternating current electric fields to manipulate fluid or particles in fluid. While typical diffusion is a slow process. ACEK can accelerate the detection and binding between targets and probes. There are three different mechanisms overall, which may happen depending on the AC signal and the solution it applies to.

2.1.1 Dielectrophoresis

The first kind of force is dielectrophoresis (DEP). It happens to the polarized particles in the solution. The geometry of electrodes can form a nonuniform electric field, causing these particles to move along with it. DEP can either repel particles of attract, based on the configuration of the particles and the solution. This can be explained through the equation of DEP force.

$$F_{\text{DEP}} = 2\pi\varepsilon_m a^3 \text{Re}[f_{\text{CM}}]\nabla|E|^2 \tag{2.1}$$

$$f_{\mathrm{CM}} = \frac{\varepsilon_p{}^* - \varepsilon_m{}^*}{\varepsilon_p{}^* + 2\varepsilon_m{}^*} \tag{2.2}$$

Variable a is the diameter of the particle. Subscription 'm' means medium, 'p' as particles. The function f_{CM} is called Clausius–Mossoti (CM) factor. Four permittivity terms within it are all complex numbers.

Since the CM factor term can be either positive or negative, showed in Equation 2.2, the direction of the force can change along with the sign of CM factor. The force can be either repelling attracting particles[2]. In brief, DEP force is dependent on particle size, frequency, and the permittivity.

$$\varepsilon_{p,m}{}^* = \varepsilon_{p,m} - j\frac{\sigma_{p,m}}{\omega} \tag{2.3}$$

2.2   AC Electrothermal Effect

Another common phenomenon showed under AC signal in solution is AC electrothermal (ACET) effect. It is caused by the resistance of the solution and the temperature gradient induced. In aqueous solution, it can be express as Equation 2.4, where τ is a time constant of dissipation factor related to the solution.

$$F_{\mathrm{ET}} = -\frac{0.0012\varepsilon}{1 + (\omega\tau)^2}(\nabla T \cdot \bar{E}) + 0.001\varepsilon|\bar{E}|^2 \times \nabla T \tag{2.4}$$

$$\tau = \frac{\varepsilon(T_{amb})}{\sigma(T_{amb})} \tag{2.5}$$

If the frequency is not too low, the second term representing the dielectric force[11], as opposed to the Coulomb force in the first term, dominates and becomes independent from the

7

frequency. In this case, ACET force, according to Equation 2.4, is supposed to be stronger in high field area.

2.2.1   AC Electroosmosis

AC Electroosmosis (ACEO) is caused by charges induced at the surface of electrodes. When the AC signal is applied, the charges change along accordingly. Usually, it produces counter-rotating vortices between two electrodes with opposing signal. ACEO appears to be stronger when the frequency is low. It is not a main consideration in this work.

2.3   Mesh Device

2.3.1   Device Structure

The device cross-section equivalent is depicted in Figure 2.1 in a 3D view. Two mesh strips are placed in a cross without touching each other. This is done by adding two spacer strips along the rims of the bottom mesh strip. The spacer is measured 75 μm. The bottom mesh is also supported by 3 layers of Scotch tape, measured 150 μm above the substrate, hence. Besides the meshes are two walls of the well where the testing sample solution is to be inject. Note that walls are a lot higher than where the top mesh strip is. This is to ensure that an effective sample source is presented during tests.

2.3.2   Review of ACEK Effect in Mesh Device

Since both DEP and ACET forces depend on the conductivity of the test solution, an small experiment is done to account for the conductivity of solution used in later experiments. From two different kind of PBS solution, one of which with the brand Gibco does not have calcium ions and magnesium ions, serial dilutions are done from the original concentration of 10x down to 0.01x. The result is obtained with a conductivity meter, plotted in Fig. 2.2. The original unit of "μS/cm" has been upscaled 10000 times to "S/m" while the number becomes 10000 times smaller.
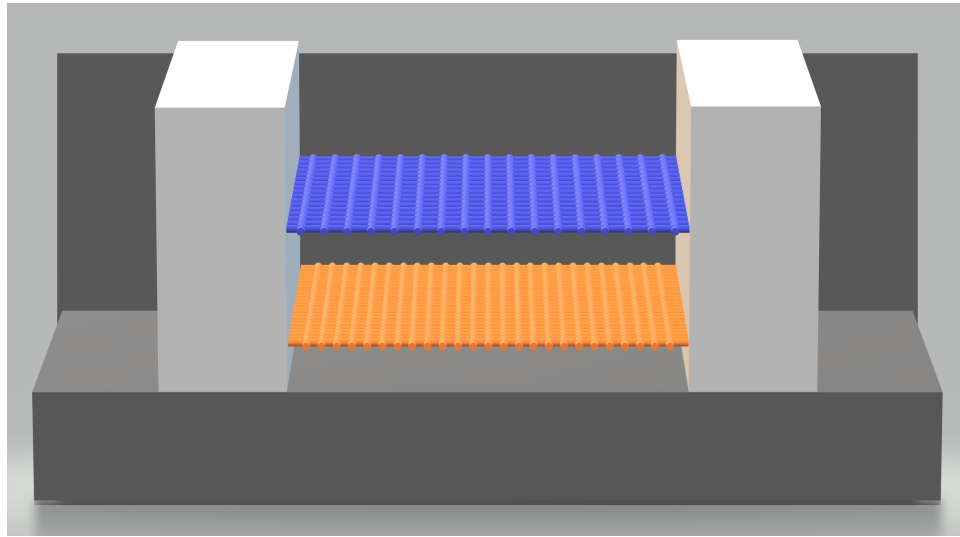
Figure 2.1: Cross-section of a mesh device in 3D. White blocks are the walls. The yellow bottom mesh is much denser than the top one.
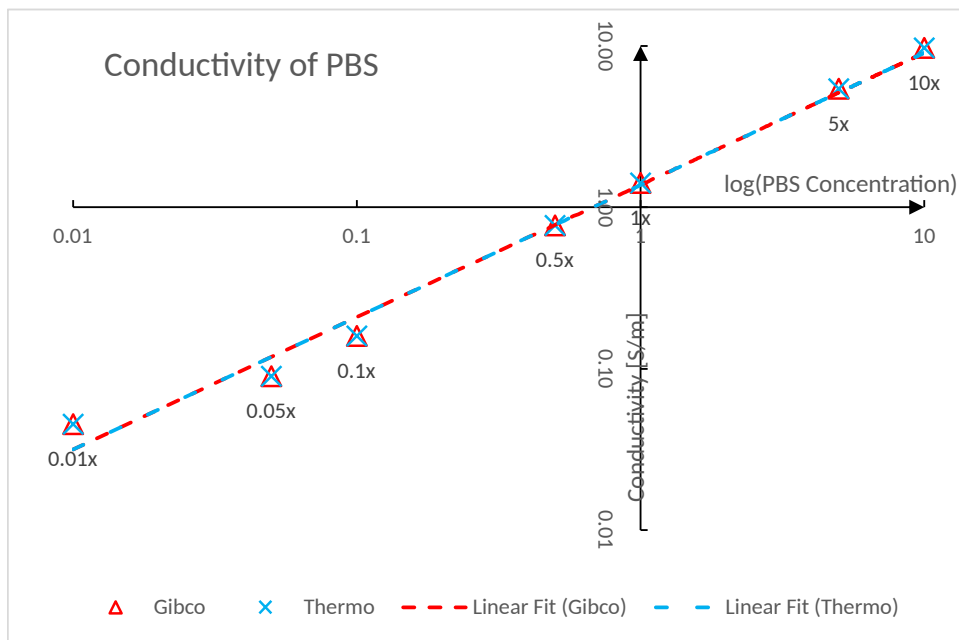
Figure 2.2: The conductivity of PBS at different concentrations (logarithmic scales).

Research on DEP

Mesh device can utilize the DEP and ACET force to create a trap between two meshes. When the salt concentration in the solution is not low, under lower frequency for viable cells, the force can be inferred as negative. Some published research supports this theory for viable mammalian cells, including RBC (red blood cells), also yeast cells and Escherichia coli (E. coli) bacteria cells, as shown in the modeling result of Fig.2.3 and the experimental data of Table 2.1.

Similar research has also been done for magnetic beads. In Figure 2.4, magnetic beads with diameter of 1 μm present to be following the nDEP. The experiment is done with both PBS (σ_m=17 mS/m) and TE buffer (σ_m=1 mS/m). As mentioned above, the least conductive solution used in this work, 0.05x PBS, has a conductivity of 0.1 S/m. The DEP force under 1 kHz of signal frequency in conductive solution exhibits the characteristic of repelling particles between wires at the bottom mesh.

Research on ACET

ACET, as mentioned above, is strongest in a triangle area formed by two bottom wires and one adjacent and parallel top mesh wire, where the electric field is also strong. It helps prevent particles from falling.

In mesh devices, the background solution must have a highest permittivity among all the testing samples. If cells above the chamber is gradually falling into it, the equivalent permittivity will gradually drop, causing a drop in its capacitance which can be measured by sensing circuits. This is how the number of cells related to the electric parameter change over a period.

2.3.3 Inference of Cell Movement Under Multiple Forces

No matter what the sizes are, all particles have gravity. It causes particles to gradually sediment. However, in an aqueous environment, particles are all susceptible to buoyancy. Particles with mass density smaller than the background solution will float to the top
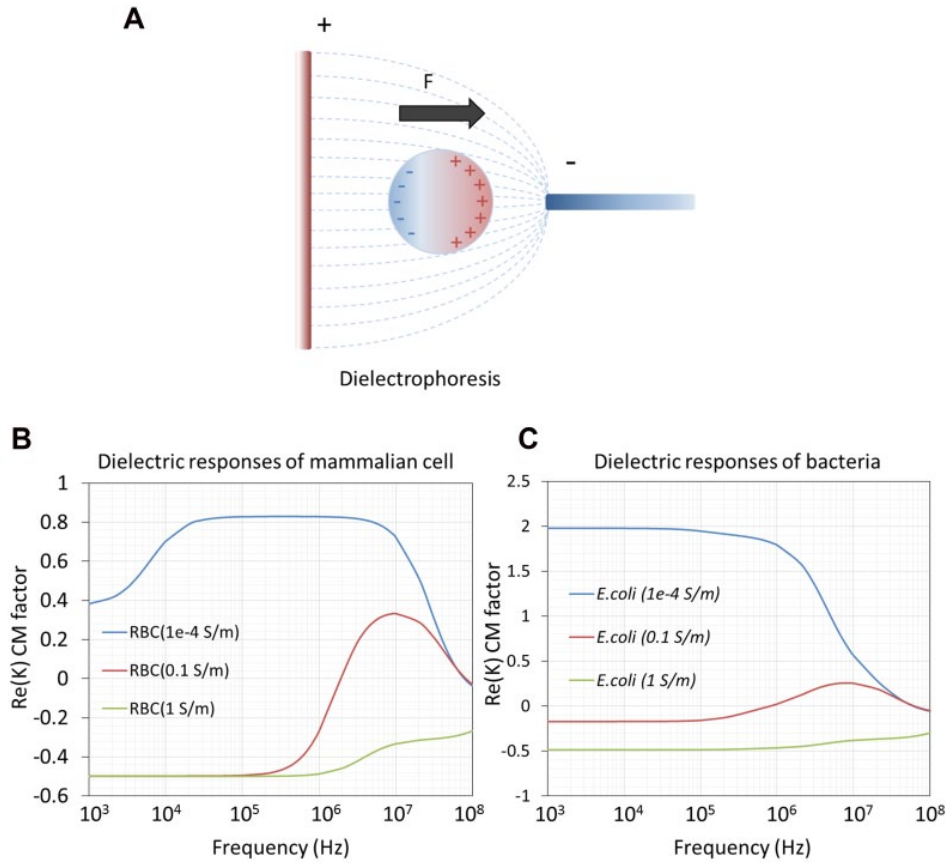
Figure 2.3: DEP mechanism (A), modeling of responses of RBC (B) and E. coli cells (C), from reference [7].

Table 2.1: DEP responses of viable and nonviable yeast cells test in solution of different conductivity, from reference [2].

Medium conductivity σ[μS/cm]	Cells	Frequency of the electric field, f [Hz]								
		1 kHz	5 kHz	10 kHz	50 kHz	100 kHz	500 kHz	1 MHz	5 MHz	10 MHz
5	Viable yeast	+	+	+	+	+	+	+	+	+
	Nonviable yeast	+	+	+	+	+	+	O	—	—
30	Viable yeast	—	—	O	+	+	+	+	+	+
	Nonviable yeast	+	+	+	+	+	+	O	—	—
78	Viable yeast	—	—	—	O	+	+	+	+	+
	Nonviable yeast	+	+	+	+	+	+	O	—	—

* □ positive response (theoretical);   + positive response (experimental);
    ▨ negative response (theoretical);   — negative response (experimental);
                    O   uncertain response (experimental).

eventually. Under these two kinds of forces, particles enter and exit the sensing area, changing the capacitance.

ACEK, in this process, tries to keep the particles from falling out of the sensing area while accelerating particles which is fast floating. Through this synergy of all forces, target particles are collecting in the sensing area very quickly. Although the bottom mesh is dense in its interlace, smaller particles can still sediment. In this way, the mesh device works like a sieve. It can help filter the unwanted and keep the targets.
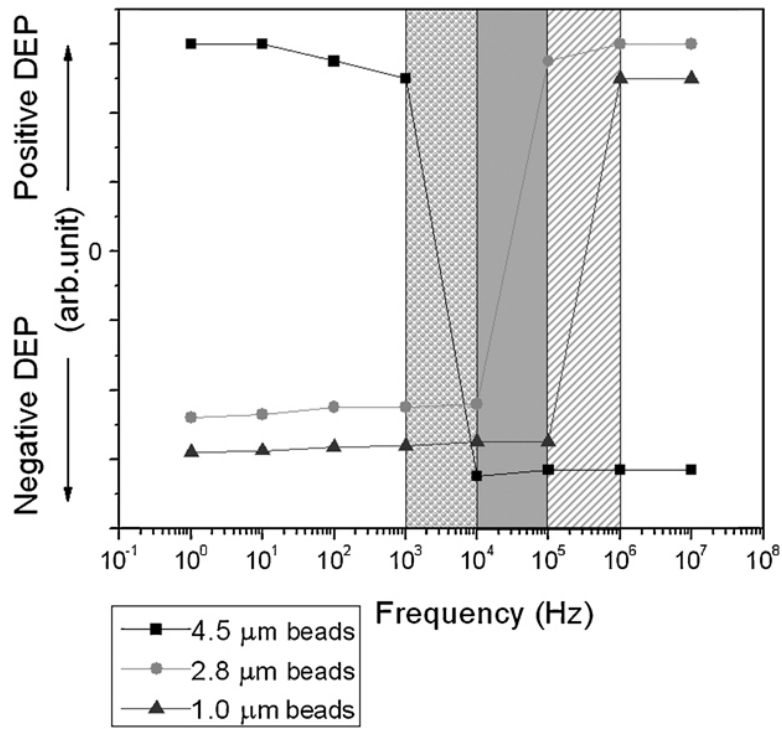
Figure 2.4: DEP responses for magnetic beads in different sizes, from reference [5].

Chapter 3

Bacteria and Particle Detection with Mesh Devices

3.1 Fabrication of Mesh Devices

3.1.1 Structure of a Mesh Device

The mesh device is built on a microscope slide. To build up the structure of the well, several layers of tapes are first set on the glass base. The thickness of one layer is around 50 μm. Theoretically, 3 layers will add up to 150 μm. The average thickness of all 3 layers measured at different position is 151.4 μm. The accuracy is good enough for the reservoir in the bottom. A 4 mm by 4 mm well is cut out with a surgical blade.

The sensor consists of a top mesh electrode and a bottom one, which are separated by layers of tapes. The bottom mesh electrode has smaller openings than the top one. Both meshes are cut from their respective mesh sheets into strips. Then they are cleaned by soaking in acetone for 15 minutes. After putting the bottom mesh on the top of the reservoir well, another layer of tape is put across and fix the bottom mesh. Excessive tapes on the edges are cut and removed. Another hole in the same size is cut out on this layer, aligned with the bottom well. Since only one layer is applied, when the top mesh is put on its top, the space between two meshes would be 50 μm. Then 3 layers of tapes are added on the top of the top mesh.

In this way, a basic and classic double-mesh structure is built out of tapes.

3.1.2   Mesh Reliability Enhancement

There are two problems in the meshes cut from sheets, causing short-circuit between two meshes. The first one is strains of loose wires sticking out of the mesh strip. They need to be trimmed before the cleaning step. The other problem is curling at the cut, which has to be solved by adding spacers at both sides of the strip, preventing curls from touching the other mesh strip.

In this work, two spacers are cut from a soft fabric tape with a thickness of 75 μm, as shown in Fig.3.1a. The layer which used to cover the whole mesh strip is now replace by two vertical tapes, fixing the mesh and spacer strips, leaving a strip area uncovered for the top mesh strip. In this way, the space between two meshes is enlarged.

The other reliability enhancement measure is applying epoxy resin at four sides and on the whole top part of the tapes, except the sensing area. With only tapes and meshes, liquid will gradually dissolve the glue under the tapes. The passage for water to get into is the gaps between tapes and meshes, and between the bottom tape and the glass substrate. The epoxy resin seals the gaps and prevent bulging when solidified. Around the sensing area, the resin can also be applied carefully to seal the inner sides of the walls.

After these two processes, the mesh device presents stable capacitance for a long period.

3.2   Method of Testing

3.2.1   Preparation of Samples

With every given target antigen to detect, there would be a type of corresponding antibody. Before the test, effective beads have to be produced first. The background solution also needs to be prepared before the mixing step. Then they can be use in the actual test.

The magnetic beads are first modified with target antibody, and then diluted to a proper concentration. The concentration of 10^7 per milliliter comes with very stable result and is used in the following tests. When the sample is ready, the beads are mixed with the obtained

15
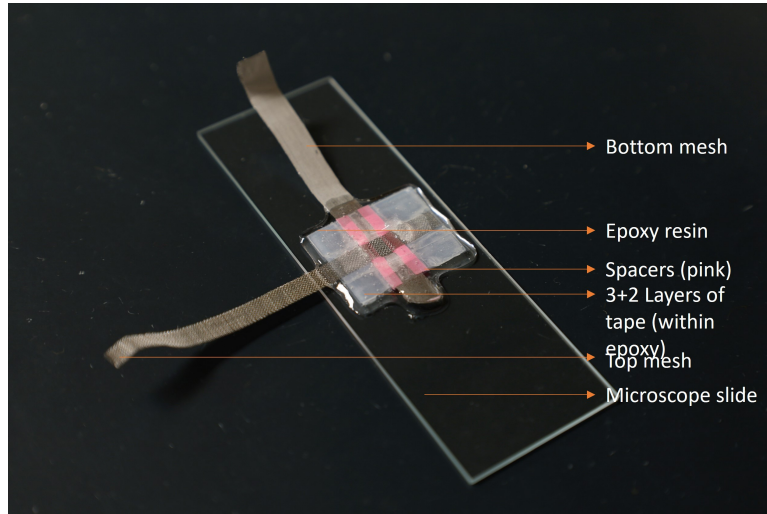
(a) Lab-made Mesh Structure
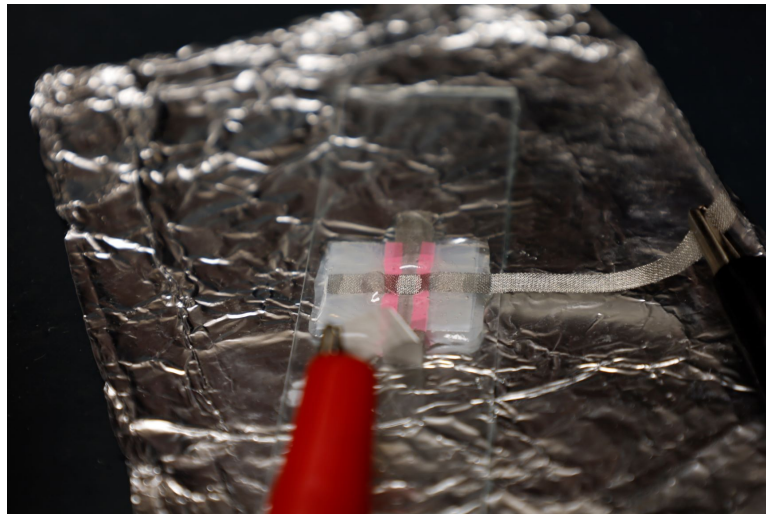
(b) Connection

Figure 3.1: Lab-made mesh device and its connection.

sample in designed background solution for 30 minutes. The background typically consists of the 0.05x PBS with 0.05% Tween-20 which can reduce unspecific bindings. While there is not any restriction for the ratio among the beads, the sample and the background solution, a volume ratio of 1:1:8 is used in yeast and bacterium tests in the next section.

When the time is up, the mixing is supposed to stop. A magnet is used to remove the solution while keeping the beads in the tube. Then the mix can be diluted to any ideal concentration. This method can even be used to concentrate the target in the sample and increase the chance of target of low concentration detected by the mesh sensor. Although the modified beads have to present before testing any sample, for the same target to detect in samples, prepared once for all, the beads and the antibody can always be used in the next turn of preparation.

3.2.2 Post-processing of Result

The test is performed using a LCR meter. Results is saved on a computer through USB cable. LCR meter can record the impedance and phase information. Based on per-minute data, the capacitance of each point as well as the change rate can be obtained. The change rate is usually calculated based on the linear fit of the per-minute data, denoted as dC/dt.

3.3 Test of Yeast Cells

Yeast is another common research target. It can be easily obtained from both the market and the lab. Yeast cells have much bigger average size. They are one of the biggest unicell microorganism that can be easily obtained or found in people's daily life. Yeast is one of the biggest unicellular lifeforms in people's daily life. Its size varies greatly, across its life and across different species. This happens when yeast consumes different quantity of nutrition. Typically, the size will not be smaller than 3 μm. This makes yeast one of the best microorganisms to test and generate signals, since it is easier to be trapped in the mesh chamber. The sample tested in this work has a diameter of around 8-10 μm.

3.3.1 Background Solution

Since the yeast used in this work is released from powder-like tiny capsules, the background solution does not need any modification to adapt to any other substance introduced from original media. Hence the background solution is simply 0.05x PBS. It is good enough to keeps the same permittivity of different concentration samples.

3.3.2 Preparation

Yeast bought from the shelve of supermarket is put onto the surface of 1 mL 0.05x PBS solution in a 1.5 mL tube. The particles will dissolve gradually and form some precipitation on the bottom of the tube. After 1 hour, the supernatant is extracted into another clean tube. They are later counted under a microscope, with some proper dilution. Based on the counted number of yeast cells, the original solution is then serially diluted down to 10^6 to 10^3 cells per milliliter.

Result Analysis

Figure 3.2 shows the whole progresses of normalized capacitance change during five different tests. Here, five tests correspond to four different concentrations of yeast cells and the background PBS solution.

From Figure 3.3, it can be noticed that yeast concentrations beyond 10^4 cells per milliliter have distinct responses from the background solution. The background response is even smaller than what it is in Figure 3.6 due to a simpler composition. Nevertheless, the responses also have a strong linear relation with the concentration. The coefficient of determination, denoted as R^2, is well above 0.9. Its sensitivity also has reached -0.186%. This proved that particles at around 10 μm could generate linear response based on the concentration. The theory of nDEP force blocking the falling cells is also validated.
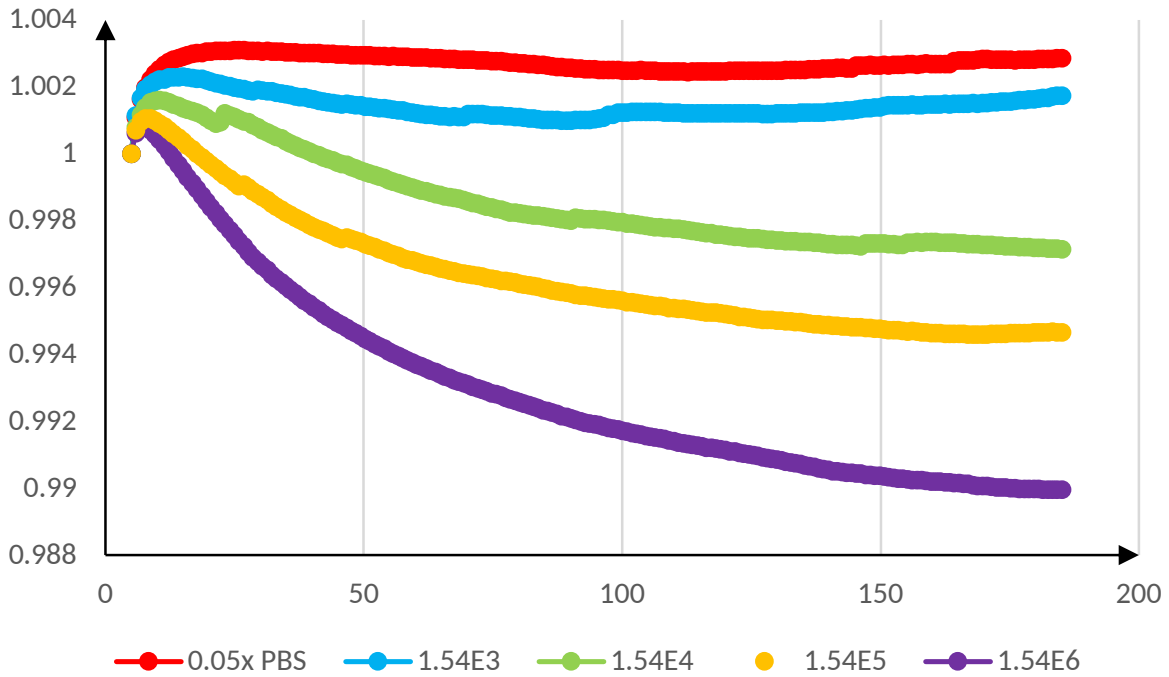
Figure 3.2: Complete 5-minute Responses of different concentrations of yeast cells.
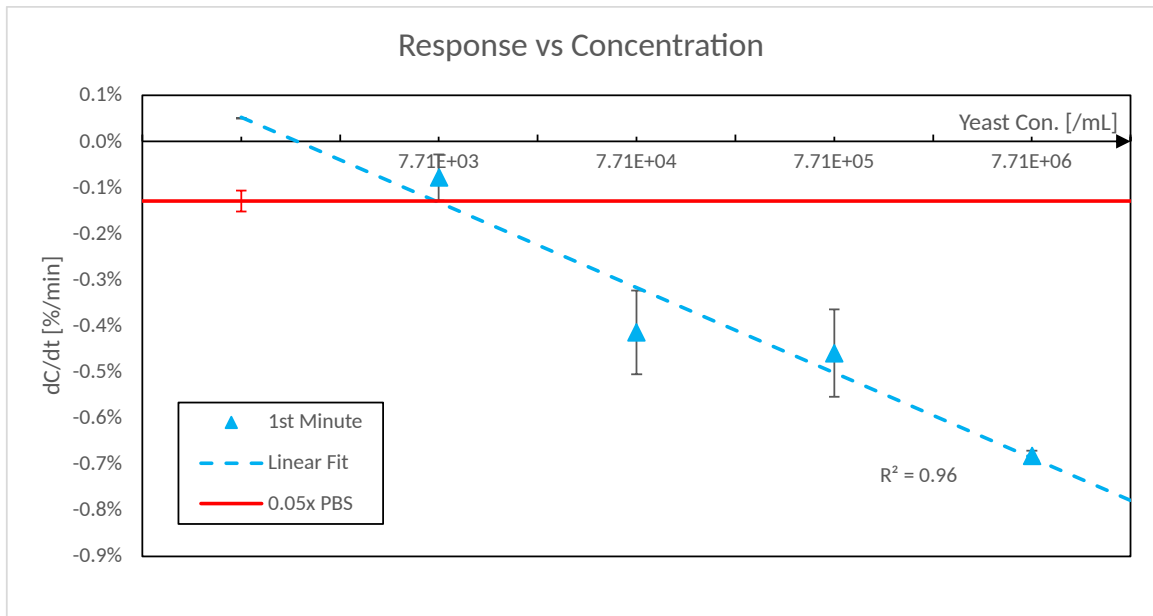
Figure 3.3: Response of different concentration of yeast cells.

19

Milk samples acquired from different sources have different conductivity. Moreover, when mixed with antibody-based beads, the background solution changes from milk to a new aqueous mixture. The conductivity can be adjusted to achieve higher sensitivity and responses.
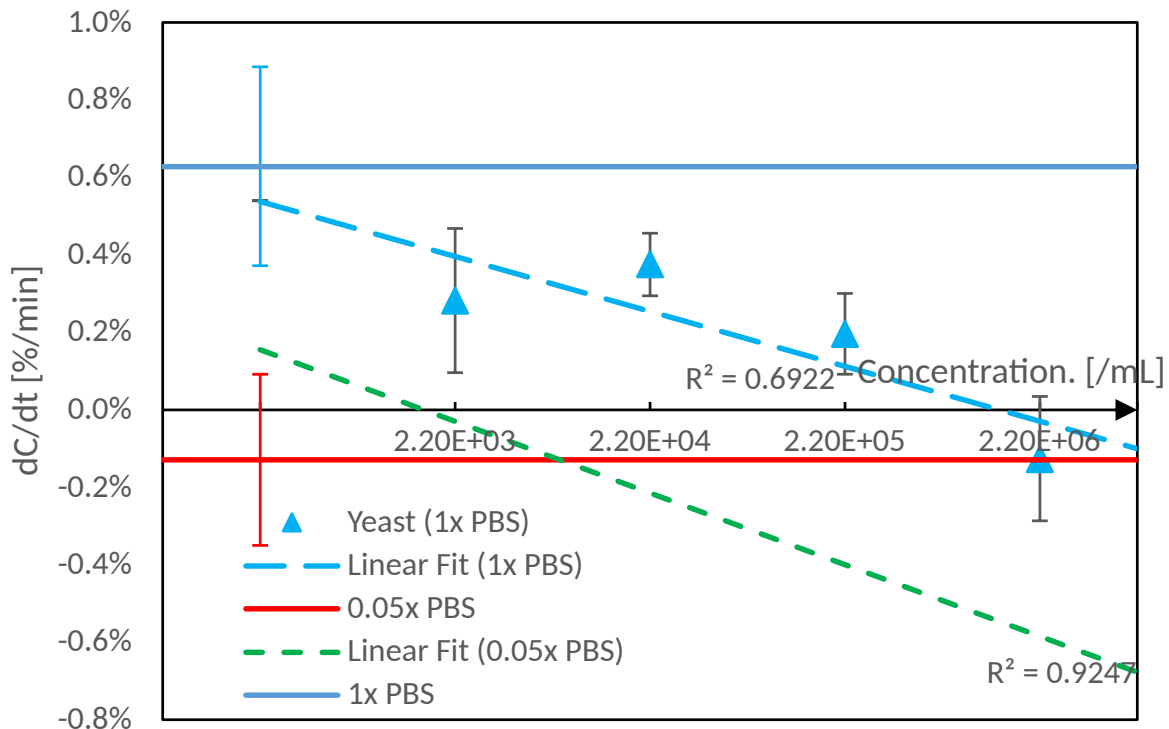
Figure 3.4: Responses of yeast in 1x PBS, compared with what is in 0.05x PBS.

3.4   Optimization

3.4.1   Ion Concentration in Background Solution

Through a yeast cell test in background solution with a different salt concentration, the responses in Fig. 3.4 give similar sensitivity results. But when yeast is in 1x PBS, the sensitivity of the mesh device is −0.14%, slightly lower than the optimized one. The result can provide guide of background concentration adjustment when the sample background is allowed to change, while solutions with different ion concentration are also acceptable by the sensor.

3.4.2   Signal Frequency and Voltage

The signal used in previous test has been optimized in respect to its voltage amplitude and signal frequency, because frequency below 100 kHz could all generate nDEP according to [5], while higher voltages have been commonly used in research as well.

Fig. 3.5a shows that the sensitivity drops drastically when the frequency goes much higher. Hence they are not considered in following tests. As for the voltage, when raised to 1.414 Vrms, the sensor can still detect yeast cells in different concentration. The sensitivity is lower but what is more worrying is the heat generated by high voltages[11].

3.5   Test of Bacterial Cells

E. coli cultivated overnight in an algae plate at 37 Celsius degree is the main bacteria source. A small portion is transferred into a cultivation solution called LB broth using a pasteurized plastic needle. After another night, a tube of bacteria solution is obtained, maximum concentration counted around 1.4×10^9 per milliliter.

3.5.1   Background Solution

Before detecting the bacteria in milk sample, it has to be ensured that they can be detected in a much simpler fluid setting first, meaning that the background solution will have nothing

21

to generate interference. A tube of 0.05x PBS solution is prepared by diluting stock 10x PBS with ultra-pure water, mimicking tap water which has a similar conductivity.

Noted that E. coli is preserved in an environment of LB broth, the ion concentration of which can severely affect the less conductive background solution aforementioned. To deal with this, a new pre-diluted bacteria source is obtained by mixing $10\mu L$ original bacteria solution into $990\mu L$ of 0.05x PBS. Spiking the tube of remaining 0.05x PBS with fresh LB solution in the same volume ratio can mimic its new background solution, accordingly, at the best effort. In background solution like this, with its ion concentration, E. coli cells are supposed to be affected by nDEP[7, 10] all right.

Later serial dilution of the bacteria is then based on the new bacteria source and the new background solution.

3.5.2   Result Analysis

But bacteria are usually too small for the mesh device. E. coli used in the lab is measured around 1 μm in diameter. They are expected to have very little responses (the red horizontal line) and no sign of concentration dependency. Figure 3.6 is the testing result of the first minute. The background solution generates responses as small as -0.2%, with some variations, because in the LB broth, there are possibly some traces of impurity. It can be inferred that the E. coli cells are repelled by the nDEP force generated by bottom mesh, but the force is too small and the opening is too big. Cells can fall right across the mesh layer to the bottom.

Definition 3.1. *Response: dC/dt, the per-minute capacitance change rate.*

Definition 3.2. *Sensitivity: The capacitance change rate $d\boldsymbol{C}/d\boldsymbol{t}$ in a decade of the logarithm to the base 10 of the linear fitted concentration line.*

The responses, dC/dt of different concentrations are all very close to the background solution response (the red horizontal line). Meanwhile, they all also fall well in the error bar of the background solution (the red error bar). The sensitivity of E. coli testing directly is calculated as only -0.032% per decade in the first minute. This means in the mesh device, particles as small as E. coli cell are not suitable as a direct testing target. However, this
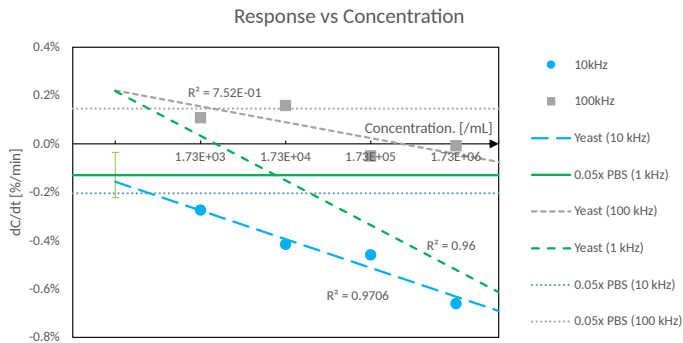
(a) 1 Vrms, 1 kHz, 10 kHz and 100 kHz
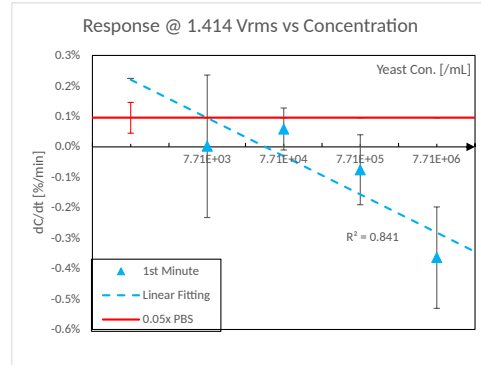
(b) 1.414 Vrms @ 1 kHz

Figure 3.5: Comparison of yeast cell responses between different voltages and frequencies.
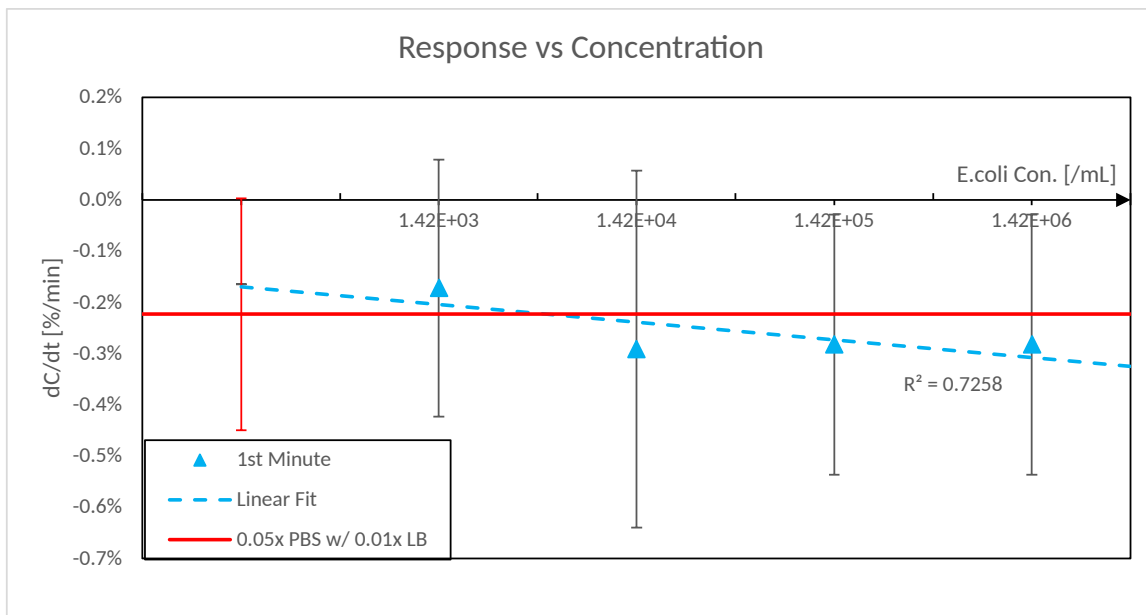
Figure 3.6: Response of different concentration of E. coli cells in the 1st minute of the test.

also means non-target small bacterial cells can not affect the detection of the target, because they can barely generate responses.

In the theory, the negative DEP (nDEP) force has a cubic dependence on the radius of the particle. With the radius going down, the nDEP force applied onto the target is diminishing drastically. Compared to a bigger cell, for example, yeast cell, it can be estimated that the nDEP force is 1000 times smaller. With the giving structure of the mesh device, bacteria tend to fall out of the bottom mesh layer on their own gravity, hardly being resisted by the nDEP force.

3.6 Binding Process and Theory

3.6.1 Overview of Bacteria-Beads Binding

To increase the target size involved with E. coli, multiple target bacterial cells should be concentrated. This can be done with antibody-modified beads. The beads are as small that they would not cause any capacitance changing in between the meshes. They also have carboxyl groups deposited on the surface. With the help of crosslinker chemical EDC and NHS, the anti-LPS (LPS short for lipopolysaccharide) antibody, which targets the major big molecule endotoxin on the cell wall of a variety of bacteria, is able to link to the surface of a bead. Both Anti-LPS antibody and anti-E. coli antibody can bind with E. coli. Among all the infection cases, E. coli is the most prevalent bacteria[3]. Using anti-LPS antibody can help accelerate the diagnosis without multiple tests.

Among different kind of beads, the magnetic ones are most convenient because they can be easily separated from any solution using a small magnet. But the most important premise is that they cannot impede the detection of the target if some of them bind well with E. coli. In the best scenario, the beads should not even generate any response.

3.6.2 Prerequisite

Since the beads and bacterium cells seen bound well, in theory, the combination should be able to detect using the mesh sensor.

24

To use the beads as a binder, as mentioned above, the response of big cells should present little difference in the process of detection. Yeast cells prepared in this experiment have concentrations 10 times higher than what they are in the previous experiment. This is because during the mixing protocol, it will be 10 times further diluted down. Beads with the concentration of 9.66×10^6, 33.3 times less than the original beads solution.

From the result, it can be inferred that this prerequisite is reached. The sensitivity is calculated as -0.125% per decade, still much higher than the scenario with only E. coli cells.

3.6.3 Visual Examination of Binding

The beads have a very high concentration when it is prepared. It has to be diluted and counted with microscopy. The concentration of a tube of beads is calculated as around 2.9×10^9 per milliliter.

After binding E. coli to the surface of the beads, the result is examined under a microscope, with a control group of pure bead solution.

With beads only, the microscopy shows that beads themselves do not bind with each other into a big cluster. The beads are distributed throughout the whole 0.1 mm thickness of the hemacytometer. Each layer is carefully examined.

The magnetic beads used in this work has a claimed diameter of 1 μm, with an even smaller permittivity compared to bacteria. But after the dilution, they should neither response to the ACEK force nor greatly changes the impedance and the capacitance of the testing solution.

3.6.4 Beads-Bacteria Binding Response

After binding with the antibody-modified beads, the beads-bacteria clusters start to generate effective response. The sensitivity is calculated around -0.151% per decade of concentration, as shown in Figure 3.9. This result resembles the one of yeast in the beads. The difference appears at the relatively higher concentrations. At the concentration of 1.44×10^5, the variation becomes large. This is when the binding happens, the uniformity of the cluster

25
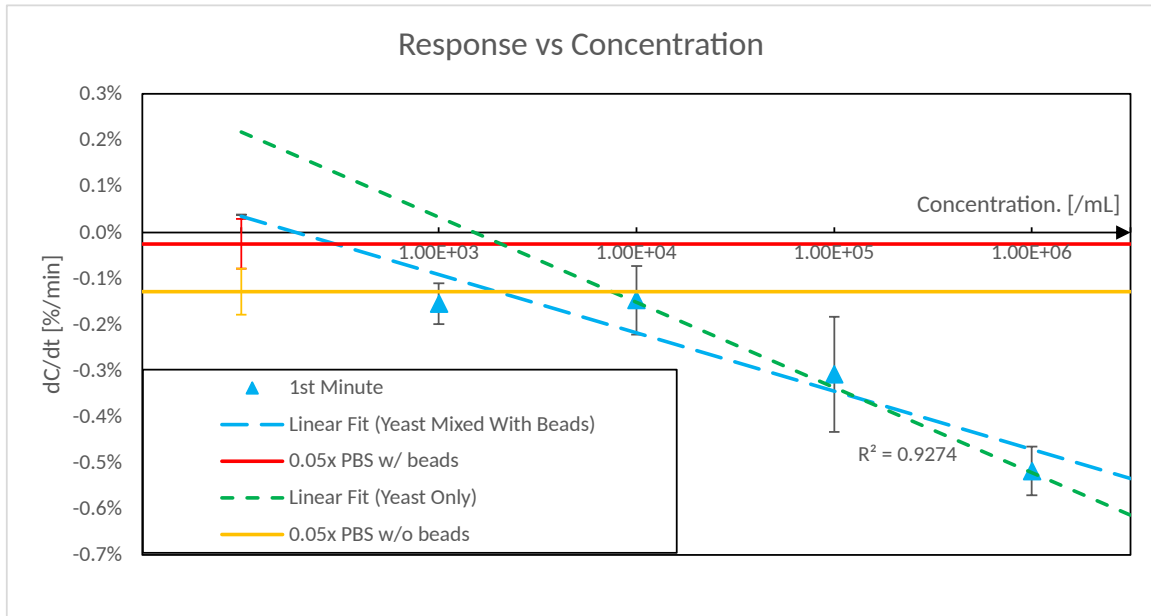
Figure 3.7: Response of different concentration of yeast cells mixed with same number of beads.

(a) Beads only   **(b)** Beads Mixed with E. coli
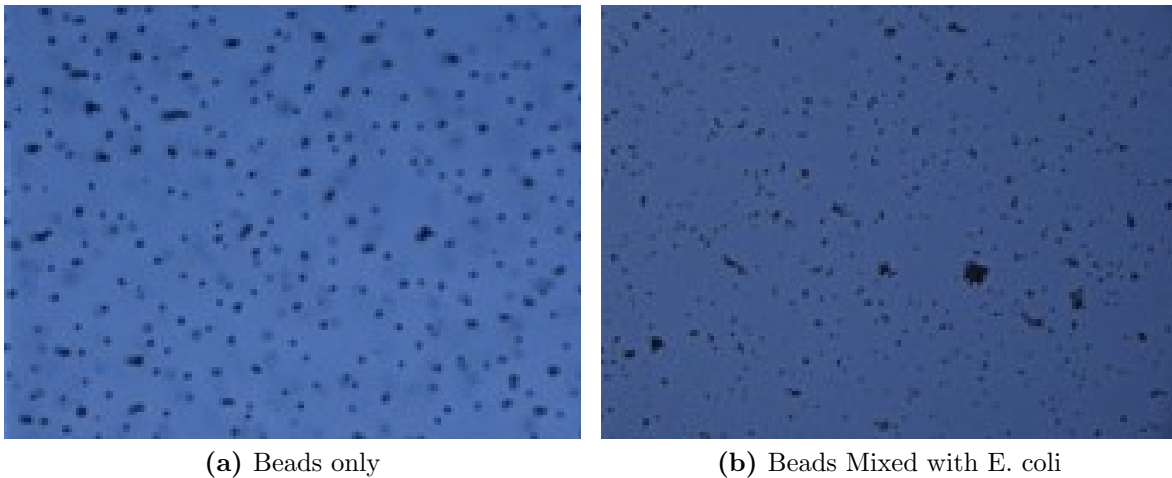
Figure 3.8: Microscopy of beads mixed with E. coli after 30-minute rocking, compared against the control group.

size cannot be strictly ensured. Rocking during the binding can mitigate this problem at certain level.

It can be inferred that it is the bacteria binding with the magnetic that forms the corresponding concentrations of clusters and generates different responses. This means the mesh device can be used with modified beads to detect certain small microorganism targets. It is versatile because the antibody linked to the surface can easily be different according to the need. Theoretically, virus like SARS-Cov-2 can also bind with the beads with the correct antibody, form clusters and be detected by the mesh device.

3.6.5 Negative Sample

The antibody used to modify the beads is targeting at a big biomolecule named "lipopolysaccharide" (LPS), present on the outer membrane of gram-negative bacteria like E. coli. In theory, the antibody is not supposed to bind with gram-positive bacteria, for example, Staphylococcus aureus (S. aureus). To verify the specificity, a negative sample test is also necessary. With the same protocol above, E. coli solution substituted with S. aureus solution, a test of different concentration of S. aureus gives the result of Fig.3.10

The responses generated by solutions with different concentration of S. aureus show little differences between samples. It can be concluded that gram-positive bacteria like S. aureus will not interfere the process of binding. Hence the binding and testing process can be target-specific, if the antibody used during modification is so.

3.7 Milk Tests

3.7.1 Lipid Influence

There are around 3% (mass/volume ratio) of fat in the milk homogenized milk product and about 5% of fat in the raw samples. Lipid forms small liquid drops due to its hydrophobic nature. In the process of sensing, lipid also goes in a different direction because its density is smaller than water. This causes the capacitance increasing gradually during the test. The

27

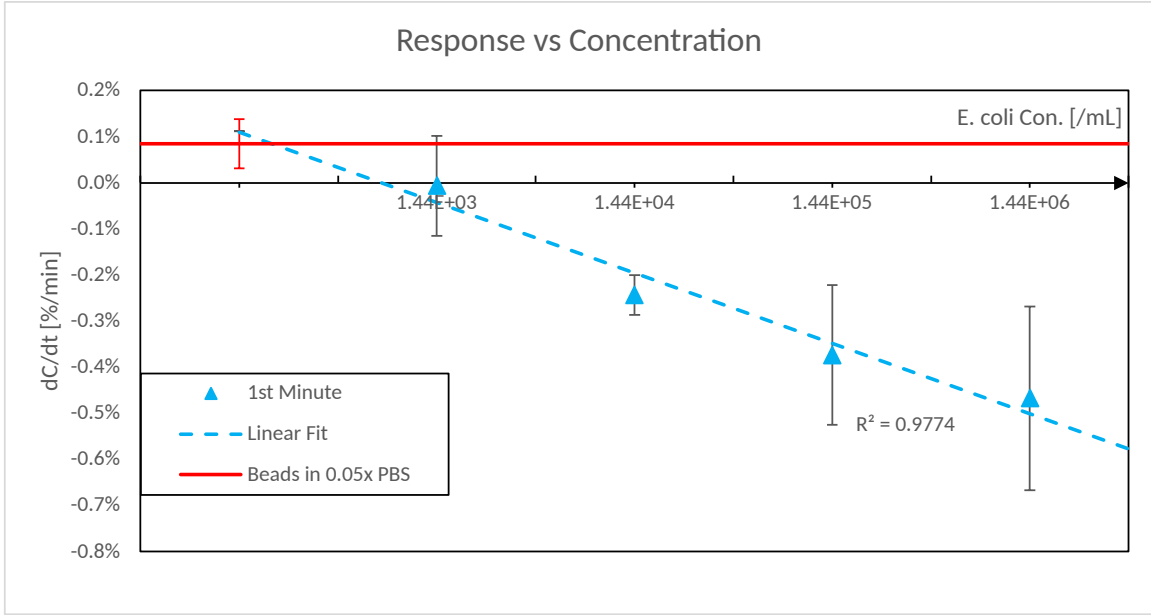**Figure 3.9:** Responses of different concentration of E. coli cells mixed with same number of beads.
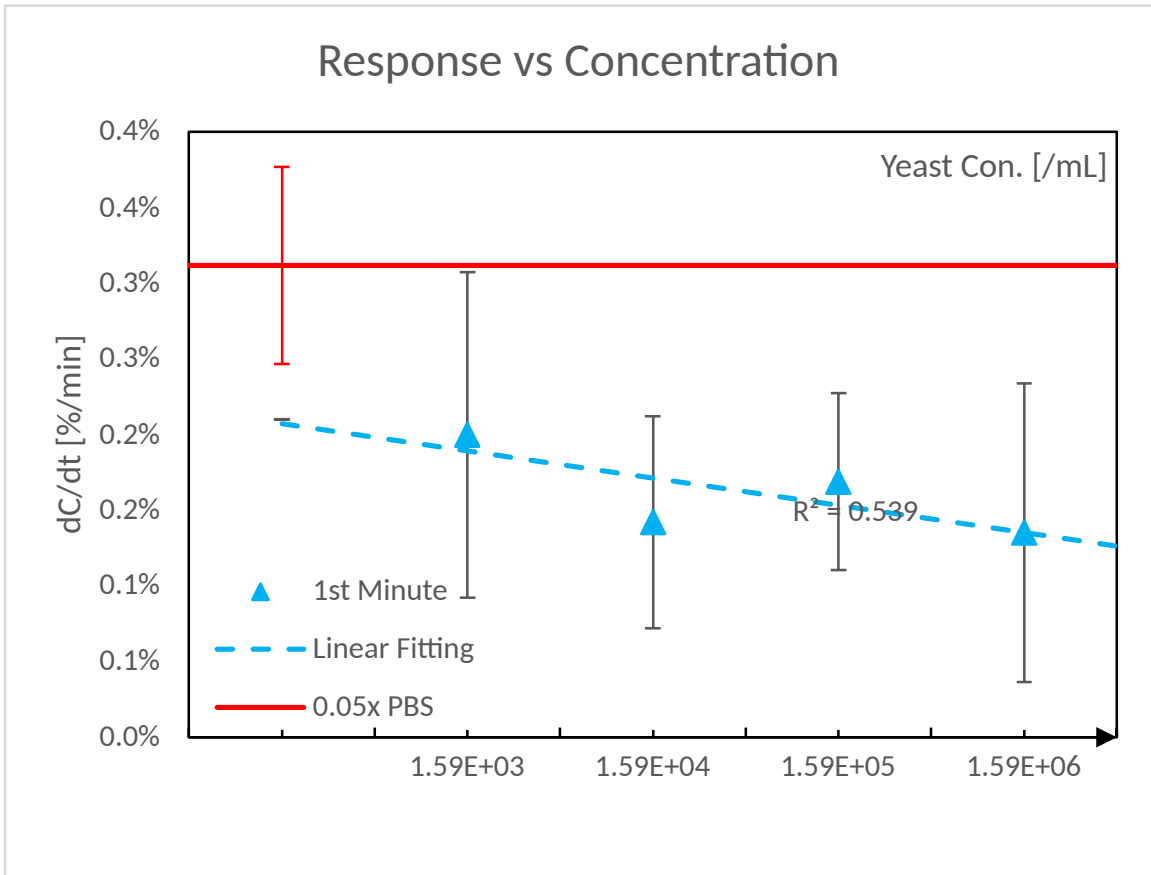
Figure 3.10: Responses of different concentration of S. aureus cells mixed with same number of beads.

size of the lipid drops is also no greater than 1 μL. In theory, lipid drops will be gradually floating out of the sensing area rather than trapped.

In a small experiment, commercial whole milk product with fat content around 3.3% is tested with mesh sensors for 5 minutes, to find out when lipids will float and leave the sensing area. In Fig.3.11, lipids have the strongest response at the first minute, meaning that they are leaving the area rapidly. The responses wane and become almost zero after the third minute. It suggests that in whole milk samples, after the fourth minute lipids cannot generate any response.

3.7.2 Raw Milk Test

Six raw milk samples coming from cows with mastitis are tested directly with mesh sensor for 5 minutes each. Fat and protein contents are measured at the origin. In Fig.3.12, the relationship between fat ration and the response is investigated for the first and second minute. Lipid drops leaving the sensing area will cause the capacitance to increase. All data points in the plot are above x-axis, proving the theory. For samples with higher fat content, the responses are higher as well. This is because with the same buoyancy, the more lipids in a sample, the more lipid drops leave the sensing area per minute. Good linear relationship is found especially in the second minute, because the electrode has been reached equilibrium in respect of surface charges. The slope of the trend lines goes down from the first to the second minute, showing that the fat content is gradually leaving and causing smaller capacitance changes.

The same data set is also used to show the relationship between the respond and somatic cells concentration. From Fig.3.13a, the relationship is rather vague. It can be concluded that lipids are the main reason for capacitance changes during this period. It does not matter how many somatic cells there are in the samples for the first minute. But at the fifth minute, Fig.3.13b, the linear relationship has been strongly built. The lipids have almost floated to the surface. The sensitivity at the fifth second is calculated as -0.0787% per decade or $-0.176\% \ F \cdot mL \cdot min^{-1}$.

In conclusion, somatic cells like white blood cells can be directly detected by the mesh device, giving that the size is around 15 μm, higher than average yeast cell size.

29
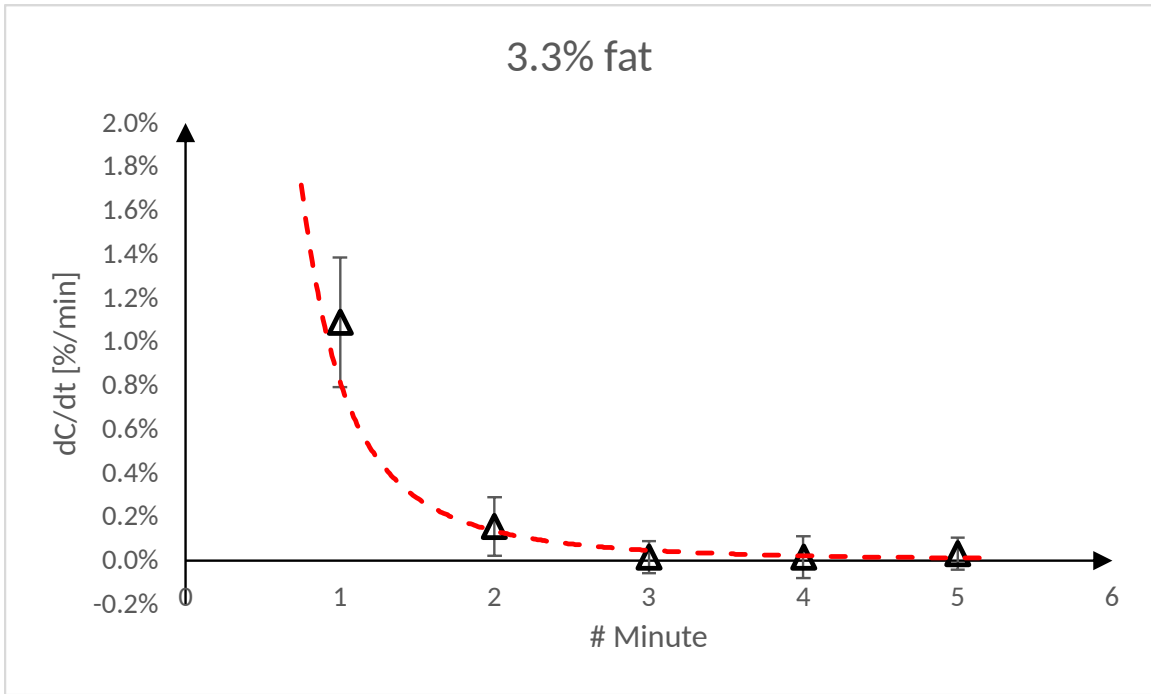
Figure 3.11: Responses of lipids in commercial whole milk product.
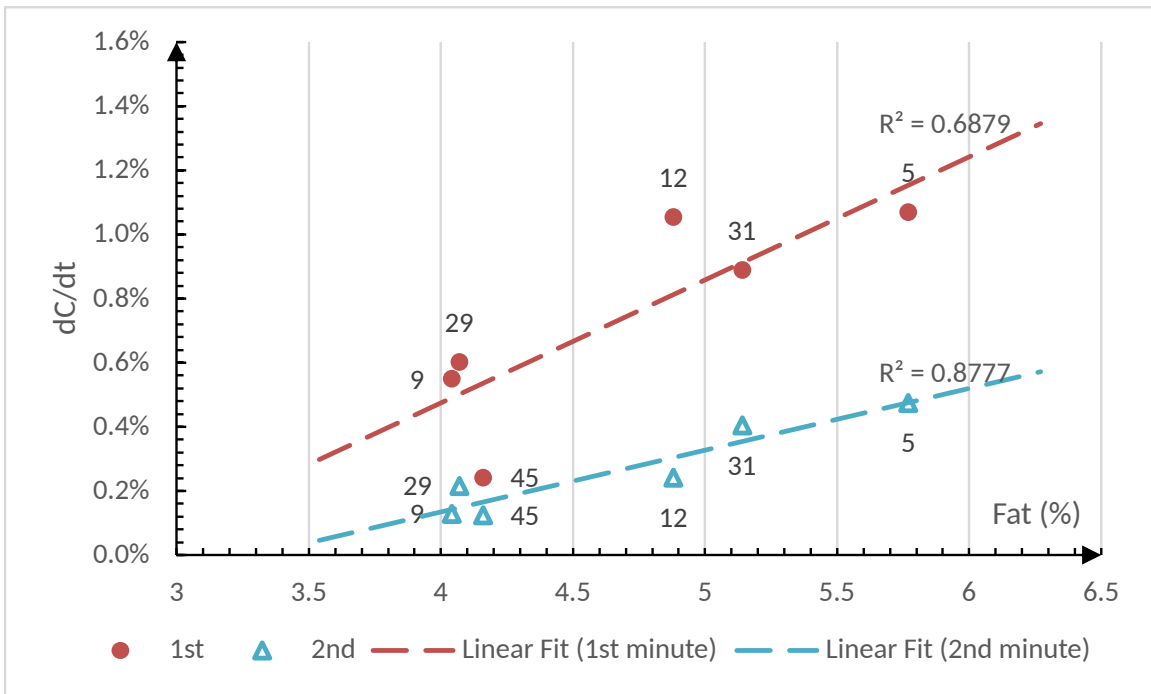
Figure 3.12: Responses of lipids in raw milk samples. (Numbers beside the markers are provided sample numbers.)

3.7.3 Bacteria-Spiked Milk Test

To simulate the milk contaminated by E. coli, commercial skimmed milk bought from supermarket is spiked with E. coli solution. The E. coli solutions have four different concentrations, 1.44×10^3, 1.44×10^4, 1.44×10^5 and $1.44E \times 10^6$. Milk is spiked with E. coli solutions in a volume ration of 9:1. New solution group is then mixed with antibody-modified beads and rocked for 30 minutes.

The result in Fig.3.14 shows that E. coli of a concentration above 1.44×10^4 in skimmed milk product can be detected by mesh device, with the help of antibody-modified magnetic beads. The sensitivity is calculated as -0.0876%, which is smaller than what is in PBS solutions. This is because lipids are not completely removed from the product. The conductivity of the mixed solution is around 0.2 S/m, which is higher than the 0.05x PBS, causing the sensitivity to decrease.

(a) 1st minute

(b) 5th minute
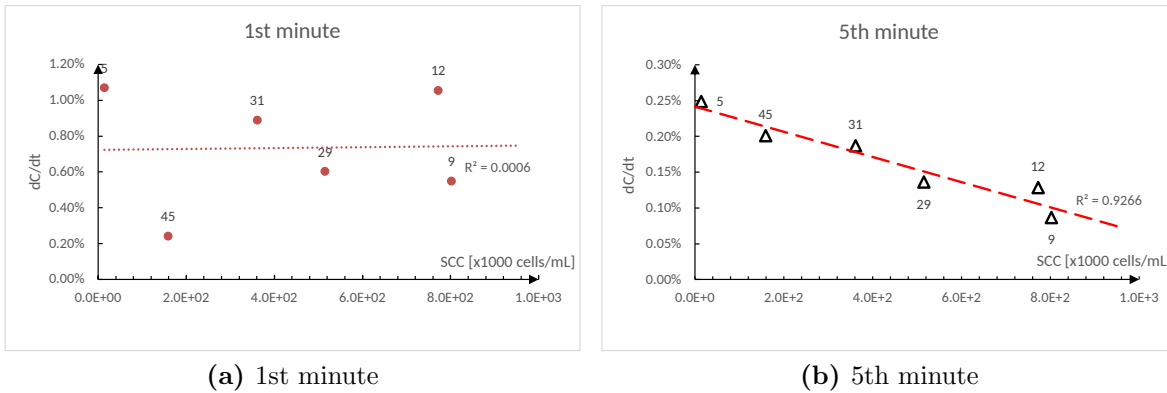
Figure 3.13: Responses of somatic cells in raw milk sample in the first and last minute.
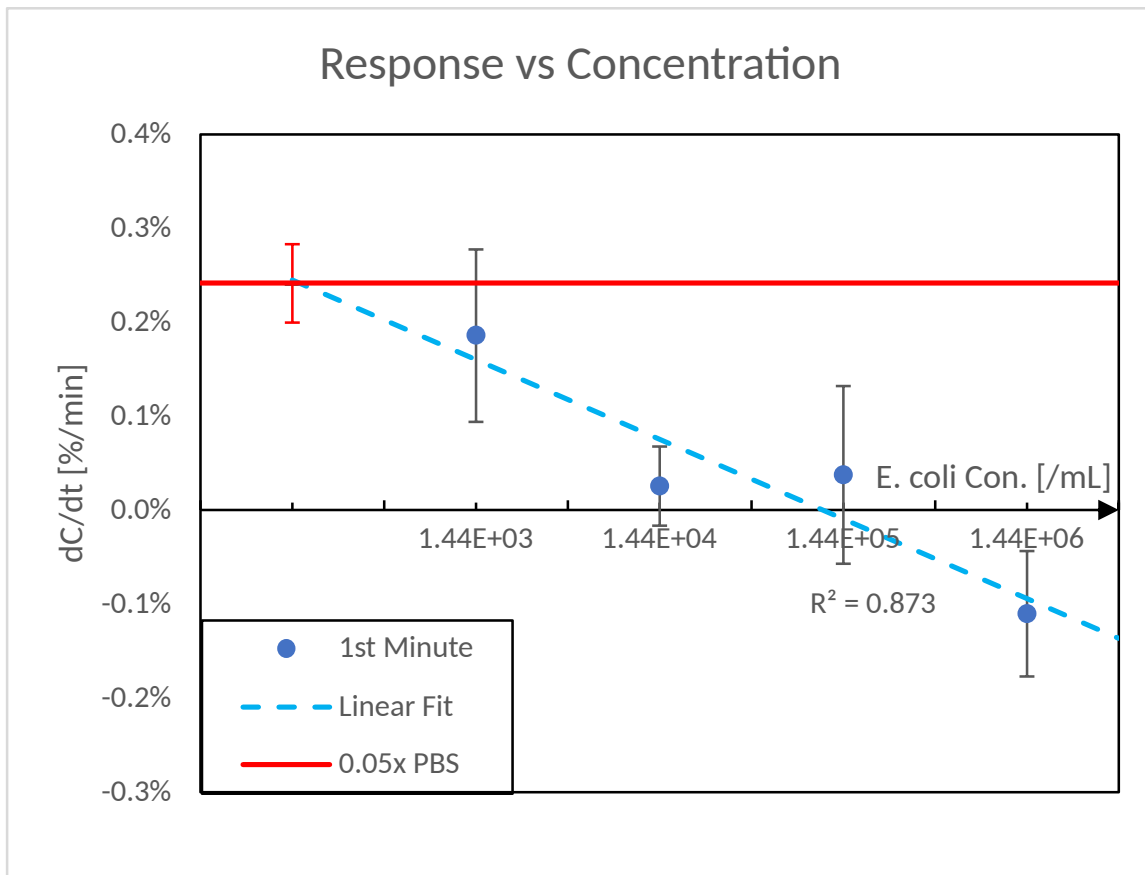
Figure 3.14: Responses of E. coli bond with antibody-modified beads spiked in commercial skimmed milk.

Chapter 4

Development of a compact embedded testing kit (aceTeK)

4.1 Circuit Considerations

4.1.1 Overview

The platform has a 32-bit ARM M3 microcontroller on a provided development board called "Mbed". It can connect with two impedance converter chips to realize the features mentioned above, in which one of them does not use a multiplexer chip at all. Chips are all powered by on-board voltage sources. Here it is 3.3 volt because the mux chip has a maximum supported voltage of 3.3 V. The span is enough for 1 Vrms test. The system has a structure as shown in Figure 4.1

4.1.2 Amplification of the Signal

The amplification is realized through the first op-amp in the signal path, with a feedback resistor. The op-amps are set up with a voltage offset at 1.67v, half of the input voltage source.

4.1.3 Attenuation of the Signal

Ingeniously, the attenuation can be implemented without changing the original circuit much. This is because one of the commonly used method to create a gain smaller than 1 using op-amps is to add a voltage division resistor in the circuit prior to the input of the fixed output signal from the chip.

To realize the voltage division, its equivalent input resistance has to be modeled. Two clamping resistors form a parallel set of resistances in AC small signal circuit. That would be the input resistance of the original circuit. Taking the advantage of this input resistance, amplitude of the signal can be divided if another calculated resistance is placed between the signal path and the ground. In this way, some part of the amplitude is dropped out of the signal path quite precisely.

This part of the circuit can also work as a buffer, even when it is at an amplification mode. To switch from attenuation to buffer mode, jumpers are in the path of the stage, to easily short the feedback resistor and choose the signal path.

4.1.4 Multiplexer and Time-Division Testing

Two I2C interfaces are supported in mbed NXP LPC1768 board. In this project, one of them is used to connect with a multiplexer chip ADG804 to expand this channel into 4, including a calibration channel. The multiplexer is supposed to have a very small on-resistance. It is crucial because the impedance of the electrode can be as small as one or several hundred ohms.

4.2 Programming

4.2.1 Calibration

The sensing circuit uses a calibration resistor to calibrate the internal phase angle. When the value of the calibration resistor is determined, the range of the testing impedance would be a small range around the value if less error is expected. Calibration resistor, which should generate 0 phase shift, can be used to eliminate the system internal phase shift. Based on

the known resistor, other impedance can be calculated through the gain factor. The gain factor is obtained at the beginning of the program through a two-point method. The code in C++ is:

```
gain_factor1 = (1 / target_impedance) / abs(Z1);    // Lower frequency
gain_factor2 = (1 / target_impedance) / abs(Z2);    // Higher frequency
gain_factor = 0.5*(gain_factor1 + gain_factor2);
```

To demonstrate the ability to measure the impedance of samples, a series of resistors are used as equivalents of different impedance of samples. They are first tested using a Keithley lab multi-meter using 4-wire sensing method. The resistance values are treated as the correct values. Then they are tested using the aceTeK platform for around 1 minute. Each result contains as many as 50 sampling points. The average value of these points is treated as the impedance measured by the platform. The percentage error is then the percentage difference between the average tested value and the correct value. By testing the series of resistors, a plot of overall error across 1000 ohms can be obtained.

4.2.2 Generation of Test Signal

AD5933 needs to be told with voltage level and frequencies to perform frequency sweep. Meanwhile, if the multiplexer is used, before any test, it needs to be switched to corresponding channel. By checking the status register 0x8F, the program can decide whether the data in the impedance registers is valid or not. After obtaining the complex impedance data, the main job is about the software, including calculating phase and capacitance. By scanning 60 points and waiting for 1 second between any two points, response data of one minute under the AC signal stimulation can be collected. The code for getting one point is listed as below.

```
while (!(status_buf & kValidData))  // Wait to finish.
        {
             status_buf = ad5933.ReadStatus();
        }
```

35

```
// STEP 6. Read values from registers.
            imag_buf = ad5933.ReadImag();
            real_buf = ad5933.ReadReal();


            Z = complex<double>(real_buf, imag_buf);


            ad5933.RepeatFreq();


            wait_ms(kWaitTime);
//sweep time is this wait time multiplied by sample points
            impedance[sample_number-1][sample_points]
                = 1 / (gain_factor * abs(Z));


            phase[sample_number-1][sample_points]
                = CalcPhase(Z, calibrated_phase);


            cap[sample_number-1][sample_points]
                = CalcCapacitance(kFreq,
                impedance[sample_number-1][sample_points],
                phase[sample_number-1][sample_points]);
```

4.3   Schematic

The schematic is exported from the Altium Designer schematic editor of this project, showed
in Fig 4.4.

In the schematic, here are two portions of the design. The upper part is the absolute
necessary portion. It consists of an impedance converter chip AD5933, an amplifier circuit
and a multiplexer chip and the Mbed MCU board. The rest of the schematic shows the
optional peripherals. They are an LCD screen and its socket and another impedance
converter chip AD5933 but without the multiplexer. These two components are extended

through the I2C bus. The second AD5933 can realize the function of testing multiple samples when continuous ACEK signal has to present on both terminals at the same time.

4.4 Prototyping

The circuit design is implemented on a prototyping bread board. In Fig.4.2, only half of the board is populated with components. Under the Mbed board, there is the multiplexer chip. The other half of the space is reserved for the sensors. There are three sockets designed to attach three sensors. Both the board and the sensor can be kept inside of the aluminum enclosure, preventing electromagnetic interference.

4.4.1 Test Result

Under the testing condition of 5 mVrms output at 100 kHz, result showed in Figure 4.3 below suggests that at value similar to the calibration resistor, the system can read out rather precise impedance of testing samples at a very small amplitude and a high frequency. This is the signal sometimes used in PCB electrode. Previous test results showed that the background solution 0.05x PBS in a 75 μm mesh device is around 400 Ω. For this reason, the calibration resistor is chosen to be a metal film 402 Ω resistor with an error of $\pm 1\%$.

In this extreme circumstance, the sensing circuit performs the best when the impedance of the testing sample is close to the calibration resistor's value. It shows that aceTeK platform has the ability of testing against normal external noises. Thus, the prototyping board is ready for test run with mesh devices and other sensors using ACEK or capacitance sensing.
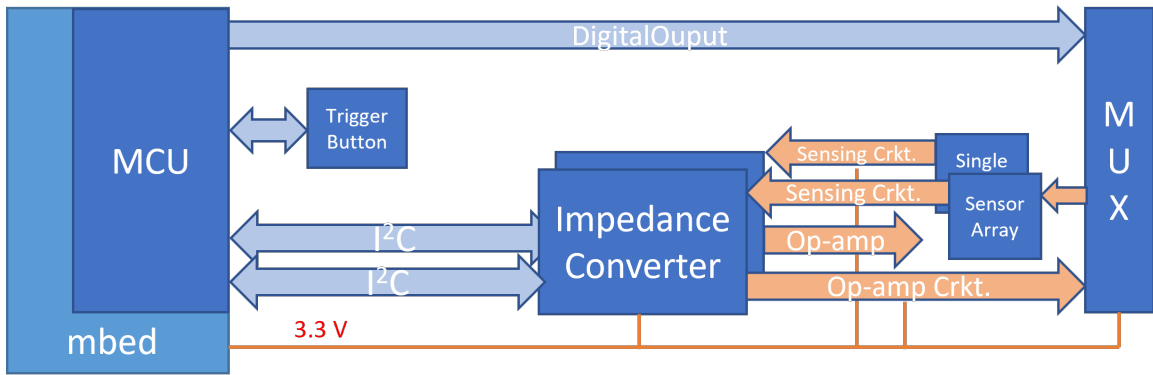
Figure 4.1: Hierarchy of the aceTeK system.

Figure 4.2: Prototype board and the enclosure.
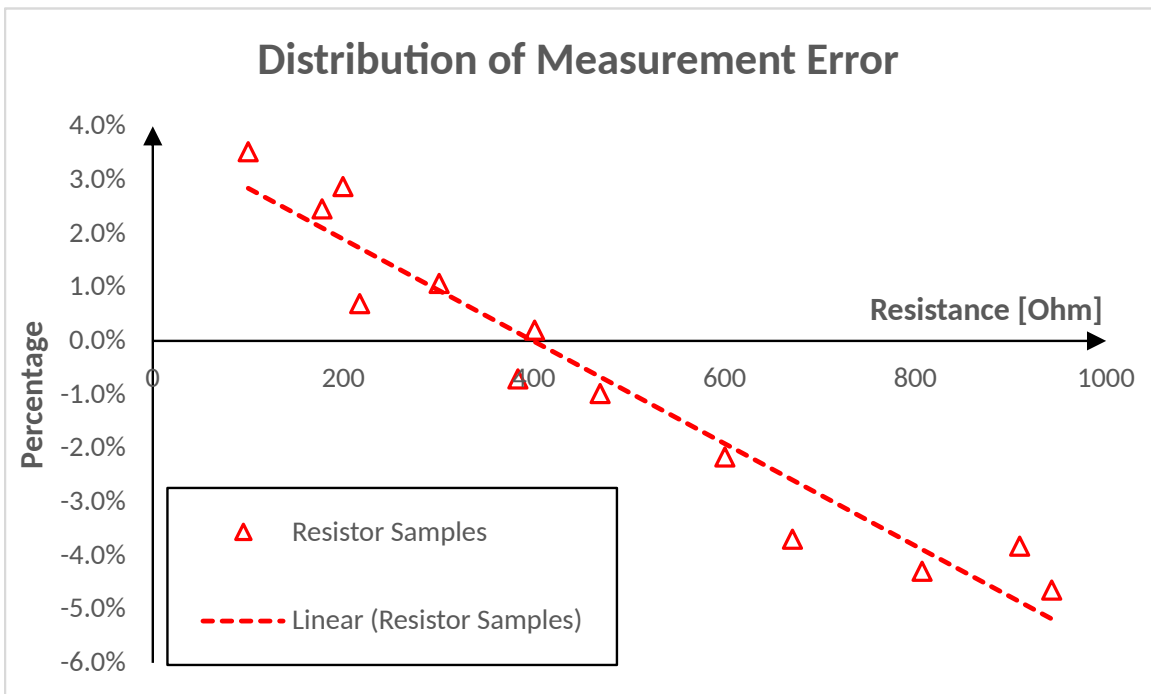
Figure 4.3: Measurement error @100 kHz 5 mVrms.
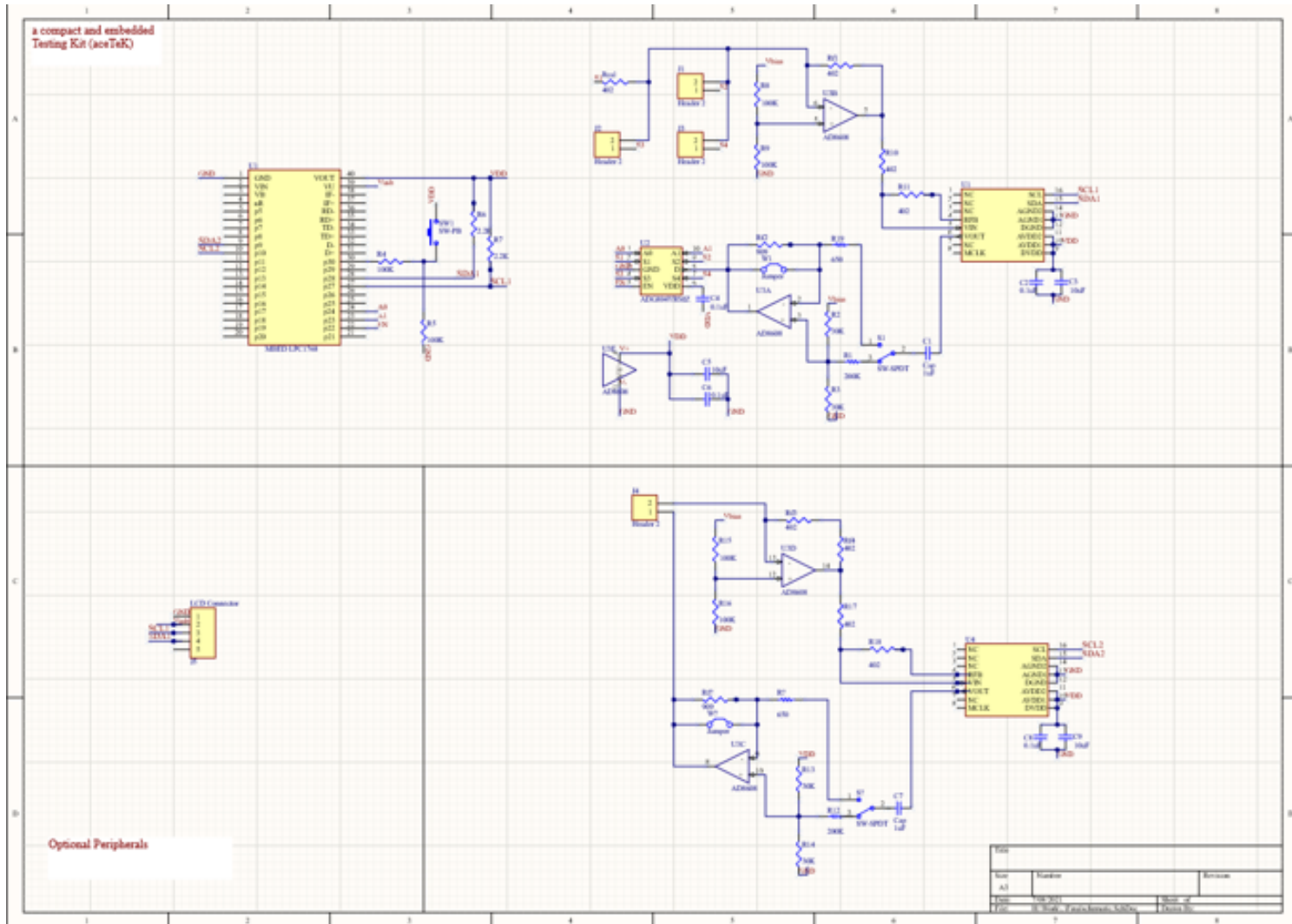
Figure 4.4: Schematic exported from the Altium Designer.

Chapter 5

Conclusions

In this work, a reusable mesh electrode is designed and fabricated. Improvement is done through structure reinforcement. The finished device is easy to perform capacitance sensing. Based on this device, ACEK effect, the theory behind the mesh device, is investigated through qualitative analysis. An experiment of yeast cell sensing proved that detection of big viable cells can be done by the sensor within 1 minute. The testing signal is optimized. With the help of antibody-modified beads, E. coli in PBS solution is also successfully detected, with good sensitivity. Its selectivity is verified through a negative sample test, which is composed of gram-positive bacteria S. aureus.

The application in milk product shows that complex solution background does not affect the performance by much. Somatic cells can be detected directly from the raw samples. This can help with the diagnosis of bovine mastitis. To further investigate the usability of magnetic beads in milk-based solution, skimmed milk spiked with E. coli bacteria is tested and analyzed. The result meets the expectation in respect of time and sensitivity.

For testing on-site conveniently, a compact testing platform is developed with the ability to output super-low voltage signals to multiple channels. It can be used to perform many kinds of capacitance sensing job at the same time, since the consideration of different kind of signal output pattern can be designed through software.

Since this method also applies to other antigens, in future work, the possibility of detecting virus can be further investigated. The magnetic beads allow to concentrate the target in samples, theoretically. A more thorough study of the optimization technique of both

the device structure and the signal properties can be done by simulation can calculation. The parameters of the meshes and the gap distance between two meshes are both very interesting topic to do further research.

Bibliography

[1] Blum, S. E., Heller, E. D., and Leitner, G. (2014). Long term effects of escherichia coli mastitis. *The Veterinary Journal*, 201(1):72–77. 1

[2] Doh, I. and Cho, Y.-H. (2005). A continuous cell separation chip using hydrodynamic dielectrophoresis (dep) process. *Sensors and Actuators A: Physical*, 121(1):59–65. ix, 7, 11

[3] Hertl, J., Gröhn, Y., Leach, J. G., Bar, D., Bennett, G., González, R., Rauch, B., Welcome, F., Tauer, L., and Schukken, Y. (2010). Effects of clinical mastitis caused by gram-positive and gram-negative bacteria and other organisms on the probability of conception in new york state holstein dairy cows. *Journal of Dairy Science*, 93(4):1551–1560. 24

[4] Jung, T., Yun, Y.-R., Bae, J., and Yang, S. (2021). Rapid bacteria-detection platform based on magnetophoretic concentration, dielectrophoretic separation, and impedimetric detection. *Analytica Chimica Acta*, 1173:338696. 2

[5] Krishnan, J. N., Kim, C., Park, H. J., Kang, J. Y., Kim, T. S., and Kim, S. K. (2009). Rapid microfluidic separation of magnetic beads through dielectrophoresis and magnetophoresis. *ELECTROPHORESIS*, 30(9):1457–1463. x, 13, 21

[6] Li, D., Feng, Y., Zhou, L., Ye, Z., Wang, J., Ying, Y., Ruan, C., Wang, R., and Li, Y. (2011). Label-free capacitive immunosensor based on quartz crystal au electrode for rapid and sensitive detection of escherichia coli o157:h7. *Analytica Chimica Acta*, 687(1):89–96. 2

[7] Lu, Y., Liu, T., Lamanda, A. C., Sin, M. L. Y., Gau, V., Liao, J. C., and Wong, P. K. (2015). Ac electrokinetics of physiological fluids for biomedical applications. *Journal of Laboratory Automation*, 20(6):611–620. PMID: 25487557. x, 11, 22

[8] Oueslati, R., Jiang, Y., Chen, J., and Wu, J. (2021). Rapid and sensitive point of care detection of mrsa genomic dna by nanoelectrokinetic sensors. *Chemosensors*, 9(5). 4

[9] Sargeant, J., Leslie, K., Shirley, J., Pulkrabek, B., and Lim, G. (2001). Sensitivity and specificity of somatic cell count and california mastitis test for identifying intramammary infection in early lactation1. *Journal of Dairy Science*, 84(9):2018–2024. 1

[10] Suehiro, J., Hamada, R., Noutomi, D., Shutou, M., and Hara, M. (2003). Selective detection of viable bacteria using dielectrophoretic impedance measurement method. *Journal of Electrostatics*, 57(2):157–168. 22

[11] Vafaie, R. H. and Ghavifekr, H. B. (2017). Configurable acet micro-manipulator for high conductive mediums by using a novel electrode engineering. *Microsystem Technologies*, 23(5):1393–1403. 7, 21

[12] Velmanickam, L., Jayasooriya, V., and Nawarathna, D. (2021). Integrated dielectrophoretic and impedimetric biosensor provides a template for universal biomarker sensing in clinical samples. *ELECTROPHORESIS*, 42(9-10):1060–1069. 2

[13] Wannapob, R., Kanatharana, P., Limbut, W., Numnuam, A., Asawatreratanakul, P., Thammakhet, C., and Thavarungkul, P. (2010). Affinity sensor using 3-aminophenylboronic acid for bacteria detection. *Biosensors and Bioelectronics*, 26(2):357–364. 2

[14] Xu, M., Wang, R., and Li, Y. (2016). Rapid detection of escherichia coli o157:h7 and salmonella typhimurium in foods using an electrochemical immunosensor based on screen-printed interdigitated microelectrode and immunomagnetic separation. *Talanta*, 148:200–208. 2

[15] Yuan, Q., Wu, J., Greenbaum, E., and Evans, B. R. (2017). A resettable in-line particle concentrator using ac electrokinetics for distributed monitoring of microalgae in source waters. *Sensors and Actuators B: Chemical*, 244:265–274. 4

Appendices

A Summary of Equations

DEP force:

$$F_{\text{DEP}} = 2\pi\varepsilon_m a^3 \text{Re}[f_{\text{CM}}]\nabla|E|^2 \tag{1}$$

$$f_{\text{CM}} = \frac{\varepsilon_p^* - \varepsilon_m^*}{\varepsilon_p^* + 2\varepsilon_m^*} \tag{2}$$

$$\varepsilon_{p,m}^* = \varepsilon_{p,m} - j\frac{\sigma_{p,m}}{\omega} \tag{3}$$

ACET force:

$$F_{\text{ET}} = -\frac{0.0012\varepsilon}{1 + (\omega\tau)^2}(\nabla T \cdot \bar{E}) + 0.001\varepsilon|\bar{E}|^2 \times \nabla T \tag{4}$$

$$\tau = \frac{\varepsilon(T_{amb})}{\sigma(T_{amb})} \tag{5}$$

B Summary of Code

B.1 On-board I/O Setup

```
I2C i2c_ch1(p9, p10);
I2C i2c_ch2(p28, p27);


DigitalOut led1(LED1);   // Create a digitalout connect to LEDs.
DigitalOut led2(LED2);
DigitalOut led3(LED3);
DigitalOut led4(LED4);


DigitalOut switch_channelA0(p24);
DigitalOut switch_channelA1(p23);
DigitalOut switch_enable(p22);


InterruptIn toggle(p30); // Create an interrupt connect to p30 for switch.
```

B.2 Main Function

```
int main()
{
//turn the Mux on and keep it on stand by mode
    switch_enable = 1;
    switch_channelA0 = 0;
    switch_channelA1 = 0;

    InitializeConverter(kVout2Vpp, kPgaGain1);
    //select the required voltage and gain
```

48

```
//the gain should be equal to 5
//  if you are dealing with low voltage configuration
    wait(1);


    //Perform sensor Calibration automatically
    ImpedanceCalibration();
    wait(1);
    //do frequency sweep across the sensor to measure impedance
    SweepImpedance();


    while (1)
        toggle.rise(&QualityControl);
        // When switch pressed, Do QC test


    return 0;
}
```

B.3   Calibration

```
void ImpedanceCalibration()
{
    FILE *file_results = fopen("/local/Results.txt", "a");


    char status_buf = 0;
    int imag_buf = 0;
    int real_buf = 0;
    double avg_imag = 0.0;
    double avg_real = 0.0;
    double gain_factor1 = 1; // GainFactor
    double gain_factor2 = 1; // GainFactor
```

49

```cpp
        complex<double> Z(0.0, 0.0);

        complex<double> Z1(0.0, 0.0);

        complex<double> Z2(0.0, 0.0);


        double target_imped = kCalibRes;


        ImpedanceConverter ad5933;   // A class of impedance converter.


        led1 = 1;

        led2 = 0;                    // Indicate the start of the sweep1

        led3 = 0;


        SwitchChannelTo(kCalibration);


    // STEP 0. Initialize the impedance converter.



        ImpedanceConverterStartFreqSweep();

        // Single point calibration with default arguments


        for (int i = 0; i < 10; i++)

        {

            while (!(status_buf & kValidData)) // Wait until DFT finish.

                status_buf = ad5933.ReadStatus();

            ad5933.RepeatFreq();

            wait_ms(kWaitTime);

            imag_buf = ad5933.ReadImag();

            real_buf = ad5933.ReadReal();

    // Compatible with 16bit and 32bit OS differences
```

```cpp
        if (kCompatibleWith16Bit)
        {
            if (real_buf & 0x8000)
                real_buf |= 0xFFFF0000;
            if (imag_buf & 0x8000)
                imag_buf |= 0xFFFF0000;
        }
        avg_imag += imag_buf * 0.1;
        avg_real += real_buf * 0.1;
    }
    Z = complex<double>(avg_real, avg_imag);
    // arg gives you a result ranging froom -pi to pi
    // with the sign based on the imaginary
    calibrated_phase = (Z.imag() < 0.0)?
        arg(Z) / Pi * 180 + 360 : arg(Z) / Pi * 180;


    avg_imag = 0.0;
    avg_real = 0.0;

    wait(1);
    ad5933.PowerDown();
    wait(1);


    led1 = 0;
    led2 = 1;                 // Indicate the start of the sweep2
    led3 = 0;

//     ImpedanceConverterStartFreqSweep(); // Single point calibration
```

51

```
    ImpedanceConverterStartFreqSweep(kFreqCali1.second);
    // Double point calibration

    for (int i = 0; i < 5; i++)
    {
        while (!(status_buf & kValidData)) // Wait until DFT finish.
            status_buf = ad5933.ReadStatus();
        ad5933.RepeatFreq();
        wait_ms(kWaitTime);
        imag_buf = ad5933.ReadImag();
        real_buf = ad5933.ReadReal();
// Compatible with 16bit and 32bit OS differences
        if (kCompatibleWith16Bit)
        {
            if (real_buf & 0x8000)
                real_buf |= 0xFFFF0000;
            if (imag_buf & 0x8000)
                imag_buf |= 0xFFFF0000;
        }
        avg_imag += imag_buf * 0.2;
        avg_real += real_buf * 0.2;
    }
    Z1 = complex<double>(avg_real, avg_imag);

    avg_imag = 0.0;
    avg_real = 0.0;

// End of single point calibration,
//  start of double point calibration
```

```
        wait(1);
        ad5933.PowerDown();
        wait(1);



        led1 = 0;
        led2 = 0;                     // Indicate the start of the sweep
        led3 = 1;


        ImpedanceConverterStartFreqSweep(kFreqCali2.second);
        // Double point calibration


        for (int i = 0; i < 5; i++)
        {
            while (!(status_buf & kValidData)) // Wait until DFT finish.
                status_buf = ad5933.ReadStatus();
            ad5933.RepeatFreq();
            wait_ms(kWaitTime);
            imag_buf = ad5933.ReadImag();
            real_buf = ad5933.ReadReal();
// Compatible with 16bit and 32bit OS differences
            if (kCompatibleWith16Bit)
            {
                if (real_buf & 0x8000)
                    real_buf |= 0xFFFF0000;
                if (imag_buf & 0x8000)
                    imag_buf |= 0xFFFF0000;
            }
            avg_imag += imag_buf * 0.2;
            avg_real += real_buf * 0.2;
```

53

```cpp
    }
    Z2 = complex<double>(avg_real, avg_imag);


    wait(1);



//    gain_factor = (1 / target_imped) / abs(Z);     // Gain Factor
    gain_factor1 = (1 / target_imped) / abs(Z1);     // Gain Factor
    gain_factor2 = (1 / target_imped) / abs(Z2);     // Gain Factor
    gain_factor = 0.5*(gain_factor1 + gain_factor2);



    fprintf(file_results, "CALIBRATION DONE!\r\n");
    fprintf(file_results, "Gain factor: %.3e, Phase: %.3f\r\n",
        gain_factor, calibrated_phase);

    char phase_lcd[16];
    int n = sprintf(phase_lcd, "%.1e, %.1e", Z1.real(), Z2.real());
    for(int i=n; i<16; i++)
        phase_lcd[i] = ' ';
//    lcd_adafruit.SendFullWord("Calibration donePress the button");
    lcd_adafruit.SendTo1stLine("Calibration done");
    lcd_adafruit.SendTo2ndLine(phase_lcd);

// STEP 8. Finished, put the AD5933 into power-down mode.
    led1 = 0;
    led2 = 0;
    led3 = 0;
    ad5933.PowerDown();
    fclose(file_results);
```

```
}


```

B.4 Frequency Sweep

```
void SweepImpedance()
{
    char status_buf = 0;
    int imag_buf = 0;
    int real_buf = 0;
    complex<double> Z;
    //Initialization of variables
    double impedance[kAmountOfSamples][kSamplePoints+1];
    double phase[kAmountOfSamples][kSamplePoints+1];
    double cap[kAmountOfSamples][kSamplePoints+1];



//    FILE *file_results = fopen("/local/Results.txt", "a");


    led1 = 1;
    led2 = 0;                 // Indicate the start of the sweep
    led3 = 0;


    ImpedanceConverterStartFreqSweep();


    led1 = 0;
    led2 = 1;
    led3 = 0;
    lcd_adafruit.SendTo1stLine("Testing...      ");
    ImpedanceConverter ad5933;      // A class of impedance converter.
// CALIBRATED! Set the loop based on how many samples need to be tested.
    for (int sample_number = 1;
```

```cpp
        sample_number <= kAmountOfSamples; sample_number++)
    {
        SwitchChannelTo(sample_number);
        wait_us(1);
        for (int sample_points = 0;
            sample_points <= kSamplePoints; sample_points++)
        {
// STEP 5. Poll status register to check if
//  the DFT conversion is complete.
            while (!(status_buf & kValidData))  // Wait to finish.
            {
                status_buf = ad5933.ReadStatus();
                led3 = 1;
            }
// STEP 6. Read values from registers.
            imag_buf = ad5933.ReadImag();
            real_buf = ad5933.ReadReal();
// Compatible with 16bit and 32bit OS differences
            if (kCompatibleWith16Bit)
                if (real_buf & 0x8000)
                    real_buf |= 0xFFFF0000;
                if (imag_buf & 0x8000)
                    imag_buf |= 0xFFFF0000;
            Z = complex<double>(real_buf, imag_buf);
            //ad5933.IncFreq();
            ad5933.RepeatFreq();

            wait_ms(kWaitTime);
            //sweep time is this wait time multiplied by sample points
            impedance[sample_number-1][sample_points]=
```

56

```
               1/(gain_factor * abs(Z));


           phase[sample_number-1][sample_points]=

               CalcPhase(Z,calibrated_phase);


           cap[sample_number-1][sample_points]=

               CalcCapacitance(kFreq,

               impedance[sample_number-1][sample_points],

               phase[sample_number-1][sample_points]);


           led3 = 0;
       }
   }
//    fclose(file_results);


   ProcessAndOutputData(impedance, phase, cap);


// STEP 8. Finished, put the AD5933 into power-down mode.
   led1 = 0;
   led2 = 0;
   led3 = 0;
}
```

Vita

Xin Xia is a Master's Candidate from the Department of Electrical Engineering and Computer Science, University of Tennessee, Knoxville. He has been studying on his Master of Science program there since 2019. Before that, he received the Bachelor of Science degree in electrical engineering from the Anhui University, Hefei, China. There, he joined the Micro/nano Electronics Laboratory, learning and doing research on anti-SEU/SET SRAM design. He also worked on computational electromagnetics with parallel acceleration. Since 2019, he has been working with Dr. Jie "Jayne" Wu as a research assistant in the field of AC electrokinetics sensing. He has experience in affinity sensors based on interdigitated electrode and dielectrophoresis sensors. His current research interests include microelectronics, digital system design, and embedded system design. He is one of the authors of a journal article published in 2020 by Dr Wu's group. He is currently working on another article based on an ACEK sensor as well.